

Off-symmetry position of interstitial muons in bismuth

G. Solt

Paul Scherrer Institute, CH-5232 Villigen, Switzerland

E. Lippelt

*Institut für Mittelenergiephysik, Eidgenössische Technische Hochschule Zürich,
c/o Paul Scherrer Institute, CH-5232 Villigen, Switzerland*

B. Delley

Paul Scherrer Institute-Zürich, Badenerstrasse 569, CH-8048 Zürich, Switzerland

(Received 22 January 1991)

The orientation-dependent second moment M_2 of the frequency distribution, observed in muon-spin-rotation experiments on a high-purity Bi single crystal below ~ 15 K and in the range of ~ 85 – 100 K, cannot be explained by the assumption that the hydrogenlike μ^+ particle is located at an interstitial inversion center in the rigid or slightly relaxing bismuth lattice; the data suggest, instead, strongly reduced muon–Bi-atom separations. While an earlier hypothesis invokes a particularly strong ($> 10\%$) lattice contraction around the implanted muon occupying one of the D_{3d} inversion sites, other alternatives are investigated here with the μ^+ particle itself displaced from the symmetry center, approaching one or more of its lattice neighbors. The present total-energy calculation for $\text{Bi}_n(\text{H})$ ($n=8$ and 32) clusters indicate that off-center binding of the H-like μ^+ particle in this structure is indeed realistic: for the muon at interstitial site 2, a particularly flat potential well, of a width of ~ 2 Å, along the crystal c axis is obtained in the unrelaxed Bi_{32} frame; allowing the inner Bi_8 shell of the cluster to relax gives rise to two minima at a distance of ~ 1.1 Å from the center, with a depth of 0.16 eV. A similar, though weaker off-center trapping at site 1, with a displacement of ~ 0.8 Å, is also indicated. The evaluation of M_2 with muon displacements near to the predicted values leads to a sensibly better agreement with the experiment for zero field as well as for transverse magnetic fields. The self-consistent molecular-orbital calculation is done by using the local-density-functional method.

I. INTRODUCTION

In recent muon-spin-rotation (μSR) experiments^{1,2} on a high-purity Bi single crystal the orientation-dependent second moment M_2 of the distribution of the magnetic field at the position of the μ^+ particle has been determined. At temperatures below ~ 15 K, where the muon is generally assumed^{3,4} to be trapped at interstitial sites, neither the angular dependence or the magnitude of M_2 allows an interpretation on the basis of a muon situated at an interstitial symmetry center in an undistorted or only slightly relaxed lattice environment; the situation is similar for the temperature range 85 – 100 K. A hint is given by the unexpected, overall *large* value of M_2 : Since broadening is caused by the fluctuating dipolar fields of the neighboring Bi nuclei, enhanced M_2 's suggest correspondingly shorter distances between trapped muons and the nearest Bi atoms. If, as a simplest assumption, the unusually large broadening was entirely due to a lattice contraction around the muon occupying a D_{3d} symmetry site, this would require¹ an *inward* displacement of ~ 10 – 12% of the nearest eight Bi atoms towards the interstitial center.

The motivation for this work was to clarify the actual atomic configuration near the muon via an *ab initio* cal-

ulation of the local electronic structure at the implanted impurity.

In a broader context, locating the muon at one of the available interstices, with possibly relaxed neighbors, is often a basic problem at the interpretation of muon-spin-rotation experiments, even in simple metals. Though for single-crystal rhombohedral bismuth the variation of the results with the orientation of the external field relative to the crystal axes^{1,2} provides a rich set of experimental data, additional and *a priori* unknown physical parameters, such as the strength and orientation of the electric field gradient coupled to the nuclei and modified by the presence of the muon, are to be assessed, besides the muon position. Therefore, *independent* theoretical knowledge concerning the energetics of the hydrogenlike μ^+ impurity in bismuth is of primary importance.

The term "lattice relaxation" is normally used to indicate the totally symmetry mode of lattice distortion around the muon at an interstitial symmetry center, of point symmetry D_{3d} for bismuth. One realizes, however, that other, less symmetric relaxation "modes" exist, which may significantly shorten some of the relevant impurity–Bi-atom distances: in these modes the *impurity* is also displaced and "trapped" at a position of lower symmetry in the interstitial cage.

Such a symmetry-reducing distortion should occur if the potential, binding the muon at the interstice, has deep enough minima outside the symmetry center. The term "off-center" will be used for such impurity positions, for which the lower point symmetry does not require the energy to have an extremum value. One has to notice that no experiment has, up to now, given evidence of static off-center positions of hydrogenlike interstitials in metals, though calculations for aluminum^{5,6} or yttrium⁷ indicated that the potential may have local *maxima*, instead of trivial minima, at some interstitial symmetry sites.

The purpose of this work is a study of the potential-energy surface in the multidimensional space of coordinates of a hydrogenlike atom and its lattice neighbors in bismuth, to find the equilibrium spatial structure and energetics relevant for the explanation of the μ SR data.

To map the energy surface for hydrogenlike impurities in metals, two main approaches are at one's disposal. The pseudopotential technique combined with "jellium" methods^{5,8,9} or recent more sophisticated effective medium theories¹⁰ take properly into account the infinite crystalline environment, but they are worked out essentially for "good" metals where, in dealing with the electronic rearrangement, the screening of the positive point charge by a homogeneous electron gas can be taken as a good "zeroth-order" approximation. Molecular or cluster calculations using *ab initio* quantum chemical methods, in turn, do not assume a linear or jelliumlike electronic response; they can deal, however, with relatively small systems so that one has either to introduce *ad hoc* boundary conditions in the attempt to simulate a bulk environment⁷ or, for free clusters, to extrapolate the result to infinitely large cluster size.⁶ The A_7 crystal structure, common to As, Sb, and Bi does not lend itself to an easy explanation by simple pseudopotentials.¹¹ Moreover, the lattice dynamics of bismuth^{12,13} indicates a complex, covalentlike electronic response to the atomic displacements, suggesting that the molecular approach, even with its limitations, may be more viable in this case. The price we pay is, of course, the limitation in cluster size, which is rather restrictive here, since the bismuth atom ($Z = 83$) itself is a "heavy" object as input for a density functional or *ab initio* electronic structure calculation.

The cohesive energy of $\text{Bi}_n(\text{H})$ clusters ($n = 8$ and 32) was calculated by "Dmol," a local density functional (LDF) algorithm for polyatomic molecules and clusters.¹⁴ Input are the atomic numbers Z_i and the nuclear coordinates \mathbf{R}_i , apart from some specifications defining the quality of the numerical approximations; the accuracy of the calculated electronic structure is limited, within the precision obtainable in the framework of the LDF, principally only by the finite size of the bismuth "frame" representing the bulk environment. The minimum of the total energy as a function of the muon position inside a cage was determined with or without allowing a displacement of the neighboring atoms. The calculated energy, when compared to that for the corresponding "empty" Bi_n cluster, gives the physically meaningful *energy of solution* for the muon at the given atomic environment.

It will be found that the binding of the muon in the two possible interstitial cages is different, and that the re-

laxation of neighboring atoms is crucial in forming a possible trapped state outside the symmetry centre. Although our mapping of the energy surface in the configuration space of coordinates is still very restricted, the static muon displacement indicated by the calculation is shown to reduce decisively the difference between the predicted and measured M_2 's.

In the next section the calculational method is shortly described, in Secs. III and IV the results for different $\text{Bi}_n(\text{H})$ clusters are discussed, Sec. V compares the predictions with μ SR experiments, and Sec. VI contains the conclusions.

II. THEORY AND METHOD OF CALCULATION

The quantity, deduced from the μ SR experiment and appropriate to test our predictions on the position and energetics of the muon, is the second moment M_2 of the distribution of the nuclear dipolar fields at the muon position.¹ For the situation where the nuclei experience both Zeeman and electric quadrupolar interactions ($I_{\text{Bi}} = \frac{9}{2}$), M_2 has the form¹⁵

$$M_2 = \hbar^2 \gamma_\mu^2 \gamma_I^2 \sum_i \left[\frac{\langle I_z \rangle_i (1 - 3 \cos^2 \theta_i)}{r_i^3} - \frac{3 \langle I_x \rangle_i x_i \cos \theta_i}{r_i^4} \right]^2 \quad (1)$$

where γ 's are gyromagnetic factors for the muon and for the neighboring nuclei with spin I and \mathbf{I} is the nuclear spin operator with component I_z along the external magnetic field \mathbf{B} . The x axis is taken to be in the plane spanned by z and the principal axis ζ of the electric field gradient $V_{\alpha\beta}$, which is assumed to be radial with the muon as centre, and θ_i is the angle between \mathbf{B} and the position vector \mathbf{r}_i of the i th nucleus; the \mathbf{r}_i 's are measured from the muon as origin and the sum goes over the relevant neighboring atoms. The symbol $\langle \rangle$ means expectation value taken for one of the energy eigenstates

$$|k\rangle = \sum_{m=-I}^I a_m^{(k)}(\mathbf{B}, V_{\alpha\beta}) |I, m\rangle$$

of the i th nucleus subjected simultaneously to the magnetic field and the electric field gradient, and the bar indicates the averaging over all of these states. In Eq. (1) and in the following M_2 is given in "frequency units," i.e., as the square of the corresponding muon precession frequency; to convert to conventional units the factor γ_μ^2 is to be omitted ($\gamma_\mu/2\pi = 13.55$ kHz/G).

One notices that the strength of the quadrupole coupling is an unknown of the problem, since the charge rearrangement around the implanted H^+ -like particle gives rise to a local, radially directed electric field gradient, which adds to the "inherent" field gradient present already in pure bismuth due to its uniaxial symmetry.

In case of zero or negligibly small external magnetic fields (i.e., when the quadrupole splitting is much larger than the shift between the nuclear Zeeman levels) Eq. (1) is not valid and the formula for the second moment $M_2 \equiv M_2^{\text{ZF}}$ in the case of odd half-integer I reads¹⁵

$$M_2^{ZF} = \frac{1}{3} \hbar^2 \gamma_\mu^2 \gamma_I^2 I(I+1) \sum_i \frac{1}{r_i^6} \left[\sin^2 \gamma_i (1 - 3 \cos^2 \theta_i)^2 + \frac{3(I + \frac{1}{2})}{4I(I+1)} (2 + 3 \sin^2 \Omega_i - \sin^2 \gamma_i (1 - 3 \cos^2 \theta_i)^2) \right]. \quad (2)$$

Here γ_i and θ_i are the polar angles of the initial muon polarization \mathbf{P} and \mathbf{r}_i , respectively, as referred to the ζ axis, and Ω_i is the angle between \mathbf{r}_i and \mathbf{P} ; for an electric field gradient directed radially away from the impurity, which will be assumed here, $\gamma_i = \Omega_i$ and $\theta_i = 0$.

One sees from Eq. (1) that the quantity M_2 , besides being a function of \mathbf{B} and $V_{\alpha\beta}$ via the expectation values, depends crucially on the relative position of the muon and the neighboring bismuth nuclei, and this dependence on \mathbf{r}_i is also explicit for M_2^{ZF} ; the main object of the present study is, precisely, to predict this spatial configuration via *ab initio* total energy calculations.

As mentioned already, finding the equilibrium configuration of the extended, periodic bismuth lattice around the muon impurity by means of the known methods of lattice statics is difficult. The binding in pure bismuth involves, besides long-range forces typical for nearly-free-electron metals, also strongly covalent features: The role of noncentral interatomic forces is important^{12,13} so that "the problem of calculating the electronic polarization [i.e., the interatomic forces] from a realistic band structure is huge."¹³ This applies *a fortiori* to a realistic model for the crystal with the implanted hydrogenlike impurity. That is why we have chosen to

study $\text{Bi}_n(\text{H})$ clusters of finite size but with a method that is not associated with any nearly-free-electron-like band structure and accounts fully for the electronic part of the total energy. The method Dmol is a local density functional (LDF) algorithm worked out for calculation of the electronic structure of molecules and metallic clusters; since its principle and functioning have been described in detail,¹⁴ only a few main features will be mentioned here. Like most quantum chemical methods, it is based on a Ritz variational expansion of the single-particle molecular orbitals (MO's) into atomic symmetry orbitals,

$$\Phi_{k,\sigma}(\mathbf{r}) = \sum c_{j,k\sigma} \phi_j(\mathbf{r}). \quad (3)$$

Here $\Phi_{k,\sigma}$ is the k,σ molecular orbital with spin σ , and the ϕ 's are appropriate symmetry determined linear combinations of orbital functions ζ_i centered at the *atoms* of the cluster; the c 's are variational coefficients. The index k and j include the symmetry character of the orbital: $k = \{n\Gamma\}$, where Γ is one of the irreducible representations of the point symmetry group of the cluster, occurring for the n th time.

The standard (LDF) approach¹⁶ is based on the self-consistent equations

$$\left[\frac{-\hbar^2}{2m} \Delta + V_s(\mathbf{r}) + \mu_{xc,\sigma}(\rho_\sigma(\mathbf{r}), \rho_{-\sigma}(\mathbf{r})) \right] \Phi_{k,\sigma}(\mathbf{r}) = \epsilon_{k,\sigma} \Phi_{k,\sigma}(\mathbf{r}), \quad k = 1, 2, \dots, \quad (4)$$

where V_s is the electrostatic potential due to the nuclei and the electron charge distribution; the substantial approximation introduced by the LDF is that the actual, generally unknown potential $\mu_{xc,\sigma}$ accounting for exchange and correlation, is assumed to depend on \mathbf{r} only through the spin densities ρ_σ ($\sigma = \pm 1$),

$$\rho_\sigma(\mathbf{r}) = \sum_k^{\text{occ}} |\Phi_{k,\sigma}(\mathbf{r})|^2, \quad \rho = \sum_\sigma \rho_\sigma. \quad (5)$$

In this formalism the total energy of the system is

$$E_t = \sum_k^{\text{occ}} \epsilon_k + \sum_\sigma \int \rho_\sigma (\epsilon_{xc} - \mu_{xc,\sigma} - V_e/2) d^3r + \sum_{\alpha \neq \beta} \frac{Z_\alpha Z_\beta}{|\mathbf{R}_\alpha - \mathbf{R}_\beta|}, \quad (6)$$

where V_e is the electrostatic potential due to the electronic charges, \mathbf{R}_α is the position vector of the α th nuclei, and ϵ_{xc} satisfies $d(\rho \epsilon_{xc})/d\rho = \mu_{xc}$. For μ_{xc} the now standard Hedin-Lundqvist approximation¹⁶ was taken.

Our main concern being the total energy [Eq. (6)] of

the clusters, it is convenient that the energy zero corresponds to the dissociated atomic state so that E_t has the direct meaning of the *energy of formation*. The variational assumption [Eq. (3)] allows a treatment of the system of Eq. (4) in the usual way, as a matrix eigenvalue problem defined by the Ritz variational basis. The calculation is iterative, the electron densities ρ_σ are redetermined via Eq. (5) at each step by the calculated Φ 's and the resulting new potential is used in the Hamiltonian [Eq. (4)] to find the next approximate set of spin orbitals Φ , until self-consistency is obtained. The algorithm uses new, efficient techniques in calculating the electrostatic potential and in performing the necessary three-dimensional integrations.¹⁴

From the atomic numbers Z_α and positions \mathbf{R}_α as input, a symmetry classified set of optimized molecular orbitals $\Phi_{k,\sigma}(\mathbf{R}_\alpha; \mathbf{r})$, filled up to a Fermi level, is found, together with the total electronic energy $E_t(\mathbf{R}_\alpha)$ for the given spatial configuration. Optionally, some or all atomic coordinates can be allowed to vary so that one can arrive at the optimum atomic configuration, corresponding

to a local minimum of the total energy, without reaching complete self-consistency for *intermediate* atomic positions. We emphasize that the boundary conditions in calculating the electronic structure are those for a free molecule, in our case for neutral $\text{Bi}_n(\text{H})$. Apart from dynamical properties such as, e.g., zero-point energy, the results for $\text{Bi}_n(\text{H})$ hold for the "isotope" $\text{Bi}_n(\mu^+)$ as well, the two notations are used equivalently throughout the paper.

The atomic basis set of spin orbitals is generated, within the same LDF formalism, at the outset, and stored in a numerically tabulated form. A double set of functions for occupied atomic orbitals, required to ensure variational flexibility as in any performing linear combination of atomic orbitals–MO approach, is realized as a "double numerical basis," composed of orbitals for the neutral atom and for some ionic states. Presently, besides wave functions for atomic bismuth, orbitals for Bi^{2+} were used, and two orbitals were taken for the H or muonium atom, with the second $1s$ state calculated for an attractive charge $Z = 1.3$.¹⁴ Since the effect of core polarization on the total energy surfaces is not important, the core orbitals up to and including $5spd$ of bismuth were taken as frozen in most of the calculations, and only the $6sp$ valence states, filled as $6s^2p^3$ in the atom, were allowed to vary.

A principally serious shortcoming of the present calculation is certainly the nonrelativistic treatment of the bismuth atoms. However, very few calculations using LDF-Dirac equations have been done up to now, mostly on small molecules. According to a recent review article,¹⁷ relativistic effects shorten bond lengths and strengthen the bonds. This would tend to strengthen the trend for the off-symmetry position of the muon seen in our calculations.

First, to check the accuracy provided by our basis for a small, bismuth containing molecule, the total energy of BiCl_3 was calculated as a function of the atomic distances. The observed values ($a_{\text{Bi-Cl}} = 2.48 \text{ \AA}$, $b_{\text{Cl-Cl}} = 3.80 \text{ \AA}$) (Ref. 18) are reproduced within $\sim 3\%$, the calculated values being somewhat larger, and the calculated total energy is accordingly somewhat too small, 9.43 eV, instead of the measured heat of sublimation 9.846 eV.

The clusters in this study are to represent the crystal environment for an implanted and thermalized muon. Pure bismuth crystallizes in the arsenic (A_7) structure,¹⁹ which is obtained from the simple cubic (SC) lattice via two small distortions: First, the cell is doubled by an alternating "internal" displacement of the hexagonal planes perpendicular to the cube diagonal and second, the rhombohedral angle is slightly decreased from 60° (Fig. 1). According to a simple chemical picture, which turns out, however, to be in substantial agreement²⁰ with the actual electronic band structure, the underlying simple-cubic lattice reflects the tendency to a plausible p^3 -type bonding of bismuth atoms, and the twofold distortion, besides removing the problem of instability of the SC structure, leads to the semimetallic electronic properties.

As for possible muon "traps" in pure bismuth at low temperatures ($T < 100 \text{ K}$), the cell-doubling structure

gives rise to two kinds of interstitial sites, both of point symmetry D_{3d} but in the center of either an "oblate" (site 1) or an oblong (site 2) rhombohedron of the eight neighboring bismuth atoms (Fig. 1). The implanted muons stop, in a random way, in one of the available interstitial cages and, after some time depending on T and on the shape and height of the energy barrier between adjacent sites, the occupation will correspond to statistical equilibrium.

Allowing the lattice to relax around the muon makes the energy minima deeper, as compared to the rigid lattice. *A priori*, however, the position of the minimum can also be shifted, and even new minima can be created by the relaxational "degrees of freedom" (self-trapping); therefore the study of the energy surface implies a simultaneous variation of coordinates for the muon and for its lattice neighbors. Although a complete mapping of the energy surface for possible "routes" would be a preliminary to locate and describe the transition to the classical diffusion regime of the light impurity, it turns out that even a restricted variation of atomic positions requires very extensive computing. Experimentally, μSR data in bismuth^{1,2} indicate localized muon states below 15 K and in the range of 85–100 K, and a transition between two different regimes of this kind.

In the calculation the bismuth frames, representing interstitial cages Nos. 1 and 2, were built symmetrically around the corresponding D_{3d} inversion centers. The muon was first put into the center of the frame and then successively displaced, within the interstitial cage, along one of three lines of lower symmetry (the c axis, one of the C_2 axes, and the line directing to a rhombic face center within a σ_d plane). Since the need in computing

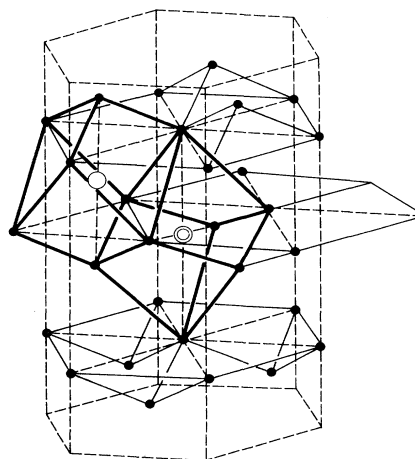


FIG. 1. View of the rhombohedral bismuth lattice. The centers of the two interstitial cages have the point symmetry D_{3d} ; \odot : site No. 1 and \circ : site No. 2. The first two neighboring shells for site No. 2 are at a distance of 2.750 \AA (six atoms) and 3.096 \AA (two atoms), the corresponding values for site No. 1 are 2.850 and 2.813 \AA . The distance between hexagonal planes alternates between 1.687 and 2.253 \AA and the rhombohedral angle is $57^\circ 17'$; the data are for $T = 78 \text{ K}$ (Ref. 19).

space and time grows by lowering the symmetry of the configuration, for larger clusters only the C_{3v} , i.e., c direction could be tested.

To minimize the influence of the “free surface” boundary condition on the calculated electronic and lattice structure in the region *near to the muon*, the cluster had to be as compact as possible. The smallest reasonable unit is obviously Bi_8 . At this, however, all the lattice atoms lie at the “surface,” therefore results for this small cluster represent, in principle, only a starting approximation. Yet, as we shall see, the energetics of the muon in this “minimum” Bi_8 frame is, in some respects, already similar to that obtained for larger frames.

The next large, compact bismuth frame is Bi_{32} with the shape of a three-dimensional cross; it is expected not only to provide a better description of the electronic structure in the central region but, by keeping the outer 24 bismuth atoms fixed, to allow also a study of the lattice relaxation around the H^+ -like impurity. Further increase of size (Bi_{56} , etc.) or a study of muon positions outside the crystal c -axis for the larger Bi_{32} cluster would require prohibitively large computational effort on the Convex machine used for these calculations.

III. RESULTS FOR $\text{Bi}_n(\text{H})$ AND Bi_n CLUSTERS

In this section the total energy calculations with different frames of type Bi_8 and Bi_{32} are summarized. Without impurity or with the impurity in the center, the point symmetry of the cluster is D_{3d} with molecular orbitals of the type $a_{1,g/u}, a_{2,g/u}, e_{g/u}$, for the reduced (C_{3v}) symmetry with H^+ or μ^+ displaced along the c axis the orbitals are of type a_1, a_2 , and e . The energy surfaces corresponding to individual orbitals of different symmetry may intersect each other, making the occupation order near the Fermi surface change as one of the atomic coordinates vary (see Fig. 2 below), which gives rise to a discontinuous change in the slope of the total ground-state energy with respect to this variable.

A. Energetics in $\text{Bi}_8(\text{H})$

The cut of the total energy surfaces E_t with the H^+ ion (μ^+) displaced along the c axis for this minimum cluster is shown in Fig. 2; in the spirit of the adiabatic approximation E_t plays the role of the potential energy determining the position and dynamics of the muon. The curves in Fig. 2 refer to Bi_8 frames taken as fixed, with shapes identical with the interstitial cages Nos. 1 and 2 in pure Bi.¹⁹ They show two important features. (i) For both cages a crossing of the two lowest-lying energy terms occurs, i.e., a change in the order of filling the orbitals as the muon position varies: with the muon at the center and near to it the ground state is found to have a degenerate orbital e as highest occupied level (the 21st of the sort, hence the notation $\{21e\}$ for this state) but, on increasing the muon displacement, the state with an orbital of symmetry a just below the Fermi level (state $\{16a\}$) will have the lower energy. (ii) E_t has a *maximum* with the muon at the D_{3d} center and two symmetrical minima for each interstitial cage, at static μ^+ displacements

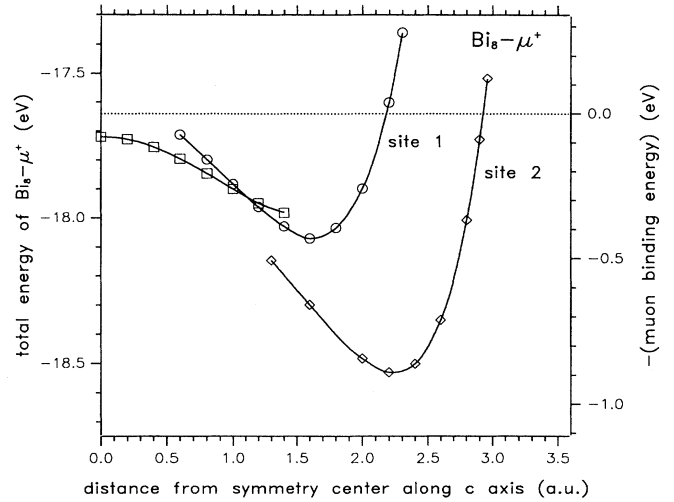


FIG. 2. Ground-state energy of $\text{Bi}_8(\mu^+)$ clusters modeling interstices Nos. 1 and 2 in rhombohedral bismuth. The muon is displaced along the crystal c axis in a fixed Bi_8 frame. The electronic term $\{21e\}$ (\square), though ground-state for a muon in and near to the symmetry center, is seen to become the first excited state for large enough displacements. The minimum for the new ground state $\{16a_1\}$ (\circ) determines the equilibrium position of the muon along the c axis. The dotted line indicates the total energy with no muon in the cluster. The lattice constants are for 78 K (Ref. 19).

$z_\mu = \pm 0.8 \text{ \AA}$ for cage No. 1 and $z_\mu = \pm 1.15 \text{ \AA}$ for cage No. 2 (the curves shown for $z \geq 0$ in Fig. 2 are invariant to $z \rightarrow -z$).

One remarks that the position and depth of the minima for the two interstitial cages correlate with the coordinates of the confining Bi atoms on the c axis: $\pm 2.81 \text{ \AA}$ for cage No. 1 and $\pm 3.10 \text{ \AA}$ for cage No. 2. Clearly, the deeper minimum for cage No. 2 is due to the larger “room” available in each of the two Bi tetrahedra, elongated in the c direction for this site.

The “energy zero” for the binding energy of the muon is the total energy of the fixed Bi_8 frame: -17.635 and -17.646 eV for site 1 and 2, respectively, i.e., -2.204 eV/atom and -2.206 eV/atom. As noted before, this is just the energy of formation of the cluster from its atomic constituents, to be compared therefore with the observed heat of formation of Bi, $E_c = 2.155$ eV.¹⁸ The calculated cohesive energy per atom is, already for this small cluster, somewhat too large, and the overestimate is only enhanced (see below) for larger clusters, with less “unbinding” contribution from surface tension. This overestimate of the binding energy is a known, systematic feature of the LDF method,²¹ but it is expected to have little influence on our conclusions related always to energy differences between appropriately chosen clusters. Interesting, indeed, is the near equality of the binding energies for clusters corresponding to sites 1 and 2: The oblate and oblong structures are energetically almost equivalent, and the same will be found for larger clusters as well.

In a similar way, the energy surface was tested along one of the C_2 axes perpendicular to c pointing towards the middle point of an edge, and also along the line within a σ_v symmetry plane, which goes through the face center of the distorted Bi_8 cube. The results for site 2, plotted in Fig. 3, show a clear minimum along the C_2 axis, at $\approx 0.87 \text{ \AA}$, and gives indication to the existence of a minimum also in the other direction, an indication only, since even if an extrapolation of the initial decrease of the curve to a larger cluster may be justified, the shape near the face center will certainly be modified by the presence of the neighboring Bi_8 cage. In fact, the shape of the σ_v curve shows only that in the $\text{Bi}_8(\mu^+)$ molecule of the given shape there is no barrier for the impurity to cross the plane of a Bi_4 surface.

Next, the position of the atoms in the Bi_8 frame was allowed to vary. The static equilibrium of Bi_8 and that of $\text{Bi}_8(\text{H})$ with fixed D_{3d} symmetry was determined, first, to see if the B_8 molecule has a shape similar to one of the crystalline cages and, second, to check if any qualitative trend to a strong inward relaxation around the central H-atom is present.

The equilibrium distances of the Bi atoms from the D_{3d} center are $l_c = 2.663 \text{ \AA}$ for the two atoms at the c axis and $l_b = 2.724 \text{ \AA}$ for each of the 3+3 atoms lying in the two horizontal planes. These are in nearly the same proportion as those for site 1 in crystalline Bi (2.813 and 2.850 \AA). Yet, considering now the distance d between the two horizontal atomic planes, the calculated value of 1.768 \AA is nearer to that for site 2 (1.686 \AA) than to the value for site 1 (2.254 \AA).

As to the ratio $\lambda = d/l_c$, equal to $\frac{2}{3}$ for an undistorted cube, the calculated value 0.664 for Bi_8 is very nearly the ideal one, right in the middle between site 1 ($\lambda_1 = 0.801$) and site 2 ($\lambda_2 = 0.545$). Thus, no sign of the internal displacement of the horizontal planes, characteristic to the

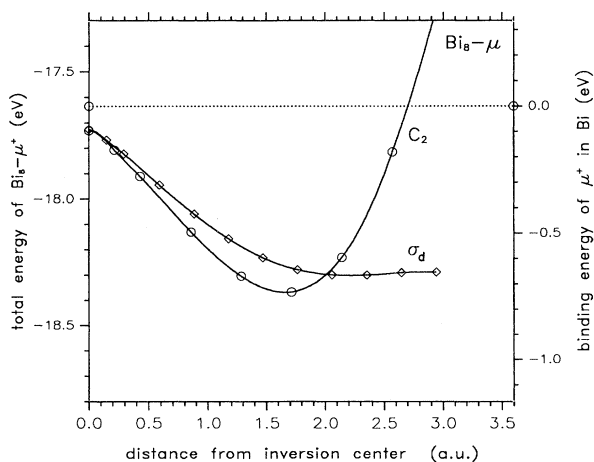


FIG. 3. Ground-state energy of a $\text{Bi}_8(\mu^+)$ cluster corresponding to interstice No. 2, with the muon displaced along a C_2 axis (toward the middle of a Bi-Bi edge) and in a σ_d plane (toward a Bi_4 face center). The dotted line indicates, as in Fig. 2, the energy of the Bi_8 cluster with no muon.

crystal, can be found in this small unit, the calculated “equilibrium” rhombohedron of Bi_8 represents a compromise between the two crystalline cages.

For $\text{Bi}_8(\text{H})$, the relaxation of the Bi_8 frame was calculated only for the case of the H atom at the center. The minimum energy occurs at a radial outward displacement of $\approx 2.5\%$ of the six Bi atoms in the horizontal planes and somewhat less for the two atoms along the c axis: no tendency, therefore, to an inward relaxation of the frame toward the impurity has been found in this cluster.

B. Energetics in $\text{Bi}_{32}(\text{H})$

By adding the next shell of 24 bismuth atoms to each of the two “central” Bi_8 frames studied above, a Bi_{32} frame of the form of a rhombohedrally distorted three-dimensional cross is obtained. Though this is still far from being a real “bulk” environment for an impurity at the center, it is expected to provide a better approximation to the shape of the muon potential for each of the two interstitial cages. Moreover, by fixing the outer shell according to crystalline order, one can allow the eight neighboring Bi atoms to relax in an environment simulating, in a first approximation, that in the solid.

First, the empty Bi_{32} frames, with sites 1 and 2 at the center, were investigated. The total energies for the frames with “crystallographical” shape are obtained to be 2.429 eV/atom for both sites 1 and 2, within the accuracy of less than 1 meV. This is by 0.2 eV/atom more than that found for Bi_8 , as a clear consequence of a smaller surface-to-volume ratio; it overshoots the observed formation energy by 0.27 eV/atom, in conformity with what has been said to this effect in the preceding section. Assuming that E_t is, approximately, a sum of volume and surface contributions of the form $E_t/V = -e_b + (F/V)e_s$, the LDF binding energy for the bulk is extrapolated to be $e_b \approx 2.75$ eV/atom. Most remarkable is that the energies for the two sites turn out to be the same within the accuracy of the calculation, as seen already for Bi_8 .

Next, $\text{Bi}_{32}(\mu^+)$ clusters with the same fixed, crystallographic frames were considered, with varying muon position. The energy surfaces, analogous to the ones in Fig. 2, are shown in Fig. 4. One sees that, in contrast to $\text{Bi}_8(\text{H})$, in the unrelaxed Bi_{32} frames no off-center minima for either site 1 or 2 occur. In turn, the curves are rather flat: That for site 2, in particular, is more of a square well than a harmonic potential. Thus, though the side minima in the potential are “leveled out” as compared to $\text{Bi}_8(\text{H})$, the roomy cages leave a large zero-point spatial extension to the impurity, for site 2 more than $\pm 1 \text{ \AA}$ along the c axis about the inversion center. For a potential surface like that shown in Fig. 4, the quantum mechanical and statistical averaging of the second moment $M_2(\mathbf{r}_\mu)$ over the muon coordinate \mathbf{r}_μ is substantial and cannot be omitted, as usually done, even in a first approximation.

Numerical methods to find the wave function for a light particle, enclosed in a potential well like that in Fig. 4 and known in all three dimensions, are available.²² However, this potential has been obtained for the undis-

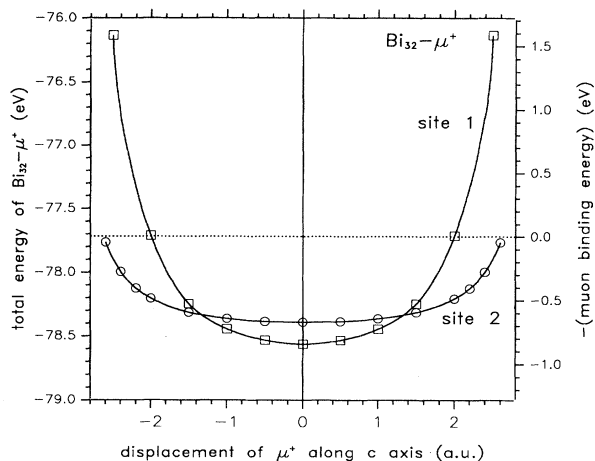


FIG. 4. Ground-state energy of $\text{Bi}_{32}(\mu^+)$ clusters, modeling interstices No. 1 (\square) and No. 2 (\circ), as a function of the muon displacement along the c axis. The Bi_{32} frame is kept fixed as in pure rhombohedral bismuth. As in Fig. 2, the dotted line indicates the total energy with no muon in the cluster. In contrast to Fig. 2, both “halves” of the potential symmetrical about the inversion center are plotted.

torted lattice and will be modified by a subsequent “optimum” relaxation of the neighbors for each given muon position, which may lead to a significant change of the $E_t(\mathbf{r}_\mu)$ curve. In fact, though the slow variation of E_t along the c axis for site 2 may be understood as a consequence of the rather distant, fixed neighbors in this direction, the constancy, within a tenth of an eV, along a range of $\sim \pm 1 \text{ \AA}$, of E_t in Fig. 4 has to be considered as accidental. One may expect, therefore, that this flatness is unstable against *any* small change in the position of the neighboring atoms, in particular, against the actual relaxation around the muon.

The amount of crystal relaxation is, however, difficult to estimate in our scheme for the following reason. Although the forces acting on the lattice atoms at their crystallographic positions are zero in the *pure crystal*, they are nonzero for a *finite cluster*, even for a hypothetically *exact* cluster calculation. Therefore, the displacements from the crystalline order are induced, in the case of the cluster, primarily not by the presence of the impurity, but by the out-of-equilibrium state of the cluster “frame” itself. This can partly, but not completely, be remedied by appropriate static constraints like the one used here: The 24 outer bismuth atoms are kept fixed at their crystallographic sites and only the inner Bi_8 cage is allowed to relax. The result of this “prerelaxation,” leading to a static equilibrium of the inner Bi_8 shell in the *empty* Bi_{32} cluster, is shown in Fig. 5. The deviation of the structure from the crystalline one occurs in a way expected already from our result on Bi_8 : The internal displacement of the hexagonal atomic planes tends to be reduced as compared to the observed value.

The λ 's for the cluster shift towards the ideal cube value $\frac{2}{3}$, for site 2 one has $\lambda'_2=0.753$ instead of

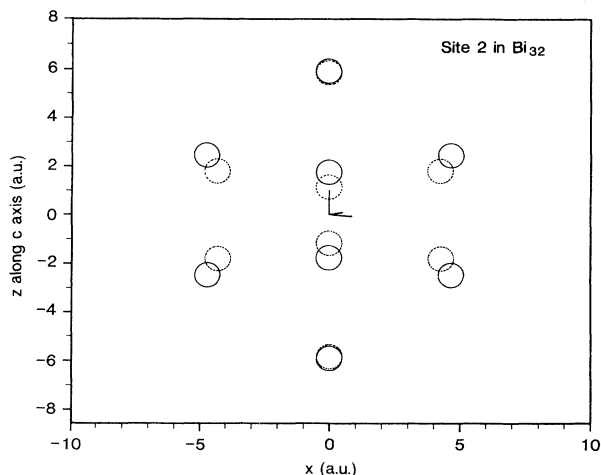


FIG. 5. The eight lattice atoms around interstitial site 2, in static equilibrium within a cluster Bi_{32} (solid circles) and in the crystal (dashed circles). For convenience, the “cube” diagonal is tilted by 10° out of the plane of the drawing.

$\lambda_2=0.545$, and $\lambda'_1=0.615$ instead of $\lambda_1=0.801$ for site 1. Unlike in the crystal, the larger λ' after prerelaxation belongs to site 2; the reason is that the fixed outer atoms confine six cages of type 1 around the central site 2, and the optimum shape of these prevails in the energy balance.

To describe now the “genuine” relaxation related to the presence of the impurity, the muon is put into the prerelaxed cluster with its inner shell in static equilibrium. The difference between the prerelaxed structure and the crystalline one, a consequence of the finite cluster size, leads however to a dramatical change of the shape of the potential as compared to Fig. 4.

The result for $E_t(\mathbf{r}_\mu)$ for $\text{Bi}_{32}(\mu^+)$, with the lattice atoms first *fixed* in the (prerelaxed) configuration of static equilibrium for Bi_{32} and then allowed to relax is shown in Fig. 6 and Fig. 7 for the two interstitial sites. For site 2, in contrast to Fig. 4, well-defined minima of E_t are seen at $z_\mu = \pm 1.1 \text{ \AA}$ of a depth of $\sim 0.16 \text{ eV}$ for both the fixed and relaxed frame. Relaxation leads to an overall energy gain of about 0.1 eV and it removes the sharp ascent of the potential at the sides via the accommodation of the repelling atom along the c axis. In the case of site 1, the relaxation of neighbors gives rise to only very shallow side minima at $z_\mu = 0.58 \text{ \AA}$, but the trend allowing more delocalization from the center is evident also for this site.

The result for the relaxed atomic positions can be summarized as follows.

(i) For site 1, the atoms relax radially outwards, typically by 2–3% for all \mathbf{r}_μ along the c axis.

(ii) For site 2 with the muon in the center, the neighbors go inwards by about 2%. At its optimal position, $z_\mu \sim 2 \text{ a.u.}$, the muon lies nearly in one of the horizontal planes of 3 neighbors; these atoms relax 1% outwards, and the nearest atom along the c axis comes nearer to the

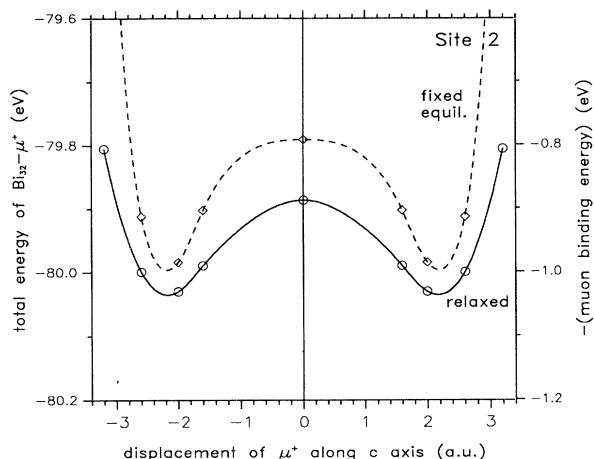


FIG. 6. Ground-state energy of $\text{Bi}_{32}(\mu^+)$ vs muon displacement for site 2, as in Fig. 4, but with the eight nearest-neighbor Bi atoms fixed in the empty-cluster equilibrium (prerelaxed) configuration (dashed line) and, also, allowing the lattice to relax at each given muon position (solid line). Relaxation leads to deeper energies and a softer rise of the curve at the sides.

muon by 0.2 a.u., which is 5% of their distance.

Obviously, Fig. 6 is *not* a proof that the H^+ -like impurity is trapped off center *in the crystal*, since the relaxed atomic configurations in the cluster differ from those in the lattice. In particular, the difference in relaxed atomic positions is *a priori* at least as large as the calculated prerelaxation in Bi_{32} *without impurity*, and this (Fig. 5) is large as compared to relaxation itself. One can, in fact, question which of the two results is a better approximation to the real potential in the *relaxed lattices*: The one obtained for the unrelaxed cluster [Fig. (4)] or the other [Fig. (6)], valid for a cage, which is relaxed as allowed by our *ad hoc* pinning of the outer 24 bismuth atoms. The implication for these two atomic configurations is clearly different: For the first, the zero-point motion of the impurity is still confined about the *center* of the cage, though with a wave function anomalously extended along

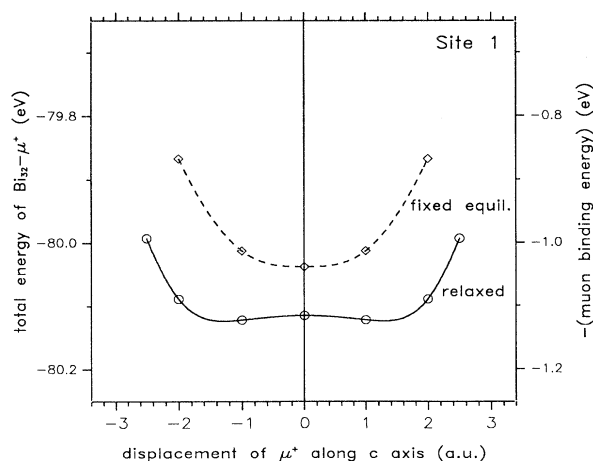


FIG. 7. Ground-state energy of $\text{Bi}_{32}(\mu^+)$ vs muon displacement in the relaxed configuration for site 1; the notation is the same as for site 2 in Fig. 6.

the c axis; for the second, the two “pockets” of the potential localize the particle above or below the inversion center. (The difference between the two cases disappears only if the average kinetic energy of the H^+ -like particle becomes comparable with depth of the side well.) With this in mind, it is safe to conclude that the calculation *excludes* a “conventional” localization of the H or μ^+ particle at the inversion center, and the off-center static trapping found in $\text{Bi}_{32}(\mu^+)$ indicates that a similar situation may be realized also in the infinite crystal.

We accept therefore, as a working hypothesis, a displaced muon position with $z_\mu \sim 1 \text{ \AA}$ for site 2 (Fig. 6) as realistic, and the possibility of a displacement at site 1, with a smaller $z_\mu \sim 0.6 \text{ \AA}$, indicated by the Bi_8 results and also in a qualitative way by Fig. 7, is also retained. On the basis of this hypothesis M_2 will now be calculated via the formulas Eqs. (1) and (2) and compared to the μSR data.

IV. COMPARISON WITH THE EXPERIMENT

A complete analysis of the experimental data, including a discussion of dependence on temperature and transverse magnetic field, will appear separately;^{2,23} here only the data for $T=11\text{K}$ are considered, where escape from interstitial trapping is assumed to be negligible.

The behavior of the expected second moment in zero external field, M_2^{ZF} , is shown in Fig. 8 for different hypothetical muon displacements along the c axis at site 2, as evaluated via Eq. (2) for the unrelaxed lattice. The shape of M_2^{ZF} as a function of the angle θ between the crystal c axis and muon polarization is indeed *qualitatively* wrong for a centrally situated muon. The shape near 90° is convex only for $|z_\mu| \geq 0.8 \text{ \AA}$, the best agreement is obtained for a displacement of $z_\mu = 0.93 \text{ \AA}$. While the calculated M_2 for a “central” μ^+ particle at site 1 is also far from the experiment, being for all angles below $\sim 0.06 \mu\text{s}^{-2}$ for the undistorted crystal,¹ a reasonable agreement can again be obtained by admitting off-center muon positions near *this* site, though with a *smaller* dis-

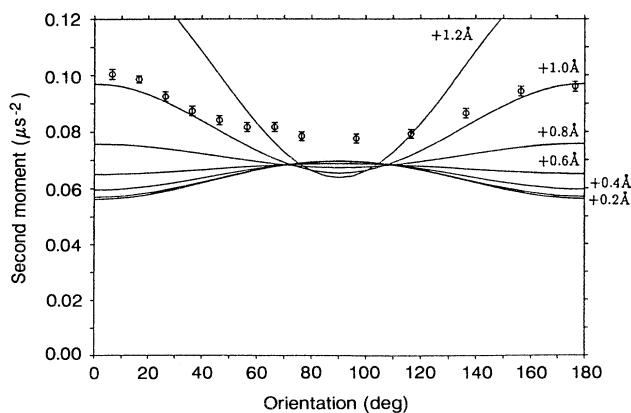


FIG. 8. Second moments M_2^{ZF} at $T=11\text{K}$ in zero external field and the calculated result for interstice No. 2, as a function of the angle between c axis and initial muon polarization. The parameter is the shift of the muon position z_μ from the symmetry center along the c axis; the lowest line is for $z_\mu=0$.

placement $z_\mu = 0.55 \text{ \AA}$, in complete agreement with the cluster results of the previous sections. In Fig. 9 the same experimental points are plotted with the "best" predictions of the theory for both sites 2 and 1.

Although the off-center potential minima have arisen as a result of lattice relaxation, the r_i 's used in Eq. (1) for calculating M_2 have been those for the undistorted crystal. The reason for this is the shift in the equilibrium atomic positions in the *cluster* as compared to those in the real *crystal*, caused by the prerelaxation discussed above; this shift is typically *larger* than the calculated relaxation, of 2–3%, from this "cluster" equilibrium. Thus, on comparing the dipolar fields with the measured signal, use of the relaxed r_i 's in Eqs. (1) and (2) would be less justified than taking the values for the unperturbed crystal. This approximation may be one of the sources of the remaining disagreement between theory and experiment in Fig. 9; another arises from an unavoidable systematic error in data processing. Experimentally, M_2 is deduced from the signal by use of a "time window" $\tau \sim 5\text{--}10 \mu\text{s}$,² the length of which is limited by resolution requirements, and the compromise in the choice of τ implies a shift in the "observed" value of M_2 . (This shift originates, in fact, in the approximate nature of the model function used in fitting the time evolution of muon polarization.²) The inset in Fig. 9 shows M_2^{ZF} for a fixed crystal orientation $\theta = 10^\circ$, plotted against τ . The difference between prediction and experiment tends to diminish with increasing τ and, though no extrapolation from the descending curve has been attempted, the true M_2 can be expected to lie fairly near to the values calculated for the off-symmetry muon positions.

Further, by looking at the potentials in Fig. 6, one can anticipate that higher temperatures lead to a smaller average muon distance from the inversion center, as a result of the occupation of excited states extending more over to the central region. This indeed corresponds to the observation.² For $T > 60 \text{ K}$ the measured angular dependence of M_2 excludes the hypothesis of muon trap-

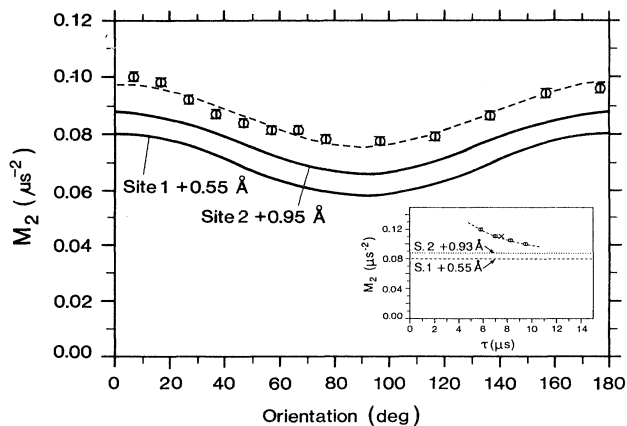


FIG. 9. Calculated second moments M_2^{ZF} for an optimum choice of muon displacements $z_\mu = 0.93 \text{ \AA}$ and 0.55 \AA for site 2 and site 1, respectively. In the inset the experimental value at $T = 11 \text{ K}$ (Ref. 2) is shown for a given crystal orientation $\theta = 10^\circ$, as deduced from the μSR signal by using different time windows τ ; \times shows the value used in earlier work (Ref. 1).

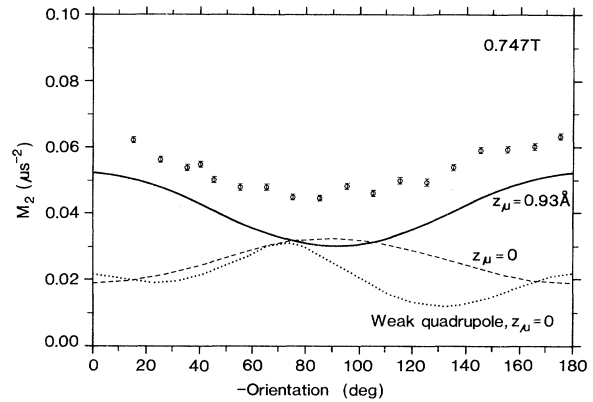


FIG. 10. Second moment M_2 in a transverse magnetic field $B = 0.747 \text{ T}$, at $T = 11 \text{ K}$, as a function of the angle θ between c axis and \mathbf{B} . The dashed line is the calculated result for $z_\mu = 0$, the solid line is that for $z_\mu = 0.93 \text{ \AA}$, assuming in both cases dominant quadrupolar interaction. For completeness, the result with the opposite assumption of weak quadrupolar coupling (dotted line) is shown for $z_\mu = 0$.

ping near site 1,² and the data at $T \sim 100 \text{ K}$ indicate an average z_μ of only $\sim 0.4 \text{ \AA}$ for site 2.

In Fig. 10 the measured data are shown for a transverse magnetic field of 0.747 T , together with the curves calculated for a central muon as well as for $z_\mu = 0.93 \text{ \AA}$. In lack of independent data for the electric field gradient generated by the presence of the impurity, the strength of the quadrupolar coupling remains a free parameter in the theory. A fit of the data on Fig. 10 has been attempted with both the assumptions of dominant or weak quadrupolar coupling of the neighboring nuclei (as compared to their Zeeman energies) for different values of z_μ . In contrast to a complete disagreement in the case of a central muon, the prediction for site 2 with $z_\mu = 0.93 \text{ \AA}$ is considerably better. Moreover, by some additional assumptions on the electric field gradient, discussed elsewhere,^{2,23} fairly good agreement with the experiment could be obtained for each value of the transverse field,² provided one takes either $z_\mu = 0.9 \text{ \AA}$ for site 2 or $z_\mu = 0.55 \text{ \AA}$ for site 1.

V. DISCUSSION AND CONCLUSIONS

The present calculations on Bi_8 and Bi_{32} clusters substantiate the hint, obtained from low temperature μSR data, that the potential for a H^+ -like impurity in bismuth does not lead to a normally expected localization at the *center* of the interstitial cage: The results indicate off-symmetry equilibrium positions along the crystal c axis. This indeed is not so surprising, in view of the following qualitative argument. First, both interstitial cages available for the H^+ -like impurity in bismuth are fairly "roomy," with eight nearest-neighbor atoms at distances of $l_i \gtrsim 2.75 \text{ \AA}$ to be compared with, for example, the twelve neighbors in aluminum with $l_i = 2.02 \text{ \AA}$ or in copper with $l_i = 1.81 \text{ \AA}$; similarly large interstitial spaces occur only in the heavier alkali and alkali earth metals. Second, cohesion in semimetallic pure bismuth has strongly covalent features, and covalency is expected to

compete with plain symmetry arguments in determining the position of the interstitial atom. As a result, the binding of a H or μ^+ particle outside the center of the spacious interstitial cage seems to be *a priori* possible or even plausible in this lattice.

The question, how adequately do the quantitative results on the finite $\text{Bi}_n(\mu^+)$ clusters reflect binding in the real *crystal*, has been discussed at various stages. We have found that the great sensitivity of the calculated potential to small distortions of the cage and the shift in the static equilibria on going from the crystal to a finite cluster make a precise prediction for the lattice very difficult. Although the *dynamical* delocalization of the impurity obtained for *unrelaxed* $\text{Bi}_{32}(\text{H})$, with a broad ($\sim 2 \text{ \AA}$) flat potential without side minima, and the static off-center positions found both for $\text{Bi}_8(\text{H})$ and for the *relaxed* $\text{Bi}_{32}(\text{H})$ clusters represent different trapping situations for low temperature, *both* imply an increased probability for the impurity to stay outside of the inversion center, a prominent feature of the results for cage 2 but, to a smaller extent, also for cage 1. (For higher temperatures and a light H isotope the difference in the two potentials becomes anyway less relevant.) Thus, without literally extrapolating one or the other cluster potential form to the solid, the cluster results certainly show that the hypothesis of an off-center trapping along the *c* axis is realistic; the indication for a static displacement of $z_\mu \sim 1 \text{ \AA}$ for site 2 is clear, the eventual off-symmetry binding at site 1 is predicted at a smaller displacement of $z_\mu \sim 0.8 \text{ \AA}$, and it has to be much weaker. The results indicate also that the self-trapping mechanism has an important role

in forming the side minima of the potential.

For the interpretation of the μSR data, values near to the cluster predictions for the static displacement are seen to lead to a considerable qualitative improvement in describing the measured orientation dependent second moment M_2 at 11 K; this can be taken as experimental evidence for off-symmetry muon positions at $z_\mu \sim 0.95 \text{ \AA}$ around site 2 and, eventually, also at $z_\mu \sim 0.55 \text{ \AA}$ around site 1 at this temperature. The data for M_2 between 85 and 100 K, indicating a reduced muon displacement at site 2, also support this model. On the other hand, no indication of an overall, significant inward relaxation of the neighboring atomic shells around the implanted particle has been obtained in any of the investigated clusters.

A study of somewhat larger Bi_n frames and a detailed three-dimensional mapping of the potential at least for $\text{Bi}_{32}(\mu^+)$ would certainly make the theoretical prediction on the position of the H or μ^+ particle more precise. For host crystals with a large atomic number, like bismuth, this requires a substantial simplification of the algorithm, possibly through a compromise of replacing the *ab initio* technique of storing or recalculating inner electronic shells at each step of iteration by a pseudopotential type of description; such development is under progress. Also, theoretical and μSR investigations of the other group V semimetals (As,Sb) with the same structure are projected.

ACKNOWLEDGMENT

The authors are indebted to Alex Schenck for several stimulating discussions.

-
- ¹F. N. Gygax, B. Hitti, E. Lippelt, A. Schenck, and S. Barth, *Z. Phys. B* **71**, 473 (1988).
- ²E. Lippelt, Ph.D. thesis, Eidgenössische Technische Hochschule, Zürich, 1990.
- ³S. G. Barsov, A. L. Getalov, V. G. Grebinnik, V. A. Gordeev, I. I. Gurevich, V. A. Zhukov, Yu. M. Kagan, A. I. Klimov, S. P. Kruglov, L. A. Kuzmin, A. B. Lazarev, S. M. Mikirtych'yants, B. A. Nikolskii, V. A. Suetin, and G. V. Shcherbakov, *Zh. Eksp. Teor. Fiz.* **85**, 341 (1983) [*Sov. Phys. JETP* **58**, 198, (1983)].
- ⁴R. Kadano, K. Nishiyama, K. Nagamine, and T. Matzusaki, *Physics Lett. A* **132**, 195 (1988).
- ⁵G. Solt, M. Manninen, and H. Beck, *J. Phys. F* **13**, 1379 (1983).
- ⁶B. Lindgren, B. Delley, and D. E. Ellis, *Hyperfine Interact.* **17-19**, 393 (1984).
- ⁷Feng Liu, M. Challa, S. N. Khanna, and P. Jena, *Phys. Rev. Lett.* **63**, 1396 (1989).
- ⁸G. Solt, M. Manninen, and H. Beck, *Solid State Commun.* **46**, 295 (1983).
- ⁹S. Estreicher and P. F. Meier, *Phys. Rev. B* **27**, 642 (1983).
- ¹⁰R. M. Nieminen and M. J. Puska, *Physica B+C* **127**, 417 (1984), and references cited therein.
- ¹¹D. Weaire and A. R. Williams, in *The Physics of Semimetals and Narrow-Gap Semiconductors*, edited by D. L. Carter and R. T. Bate (Pergamon, New York, 1971).
- ¹²E. G. Brovman, Institute of Atomic Energy Report No. IAE-1456, Moscow, 1967 (translated, Los Alamos Report No. LA-TR-68-33, 1968).
- ¹³R. E. MacFarlane, in *Physics of Semimetals and Narrow-Gap Semiconductors*, edited by D. L. Carter and R. T. Bate (Pergamon, New York, 1971).
- ¹⁴B. Delley, *J. Chem. Phys.* **92**, 508 (1990).
- ¹⁵A. Schenck, *Muon Spin Rotation Spectroscopy. Principles and Applications in Solid State Physics* (Hilger, Bristol, 1985).
- ¹⁶For a recent review see, e.g., R. O. Jones and O. Gunnarsson, *Rev. Mod. Phys.* **61**, 689 (1989).
- ¹⁷T. Ziegler, J. G. Sniders, and E. J. Baerends, in *The Challenge of d and f Electrons; Theory and Computations*, edited by D. R. Salahub and M. C. Zerner, ACS Symp Series No. 394, 1989, p. 322.
- ¹⁸*Handbook of Chemistry and Physics*, 61st ed., edited by R. C. Weast and M. J. Astle (CRC Press, Boca Raton, 1980).
- ¹⁹R. W. G. Wyckoff, *Crystal Structures* (Interscience, New York, 1960), Vol. 1, p. 32.
- ²⁰M. H. Cohen, L. M. Falicov, and S. Golin, *IBM J. Res. Develop.* **8**, 215 (1964).
- ²¹E. Wimmer, A. J. Freeman, C.-L. Fu, P.-L. Cao, S.-H. Chou, and B. Delley, in *Supercomputer Research in Chemistry and Chemical Engineering*, edited by K. F. Jensen and D. G. Truhlar (ACS, Washington, D.C., 1987).
- ²²M. J. Puska and R. M. Nieminen, *Phys. Rev. B* **29**, 5382 (1984).
- ²³E. Lippelt, P. Birrer, F. N. Gygax, B. Hitti, A. Schenck, and M. Weber, *Hyperfine Interact.* **64**, 477 (1990); (unpublished).